JOURNAL OF VIROLOGY, Apr. 2008, p. 4125–4134 Vol. 82, No. 8
0022-538X/08/$08.00+0 doi:10.1128/JVI.02232-07

Two Amino Acid Substitutions within the First External Loop of CCR5 Induce Human Immunodeficiency Virus-Blocking Antibodies in Mice and Chickens▽†

Claudia Pastori,[1] Alberto Clivio,[2] Lorenzo Diomede,[1] Roberto Consonni,[3] Giacomo M. S. De Mori,[4] Renato Longhi,[4] Giorgio Colombo,[4] and Lucia Lopalco[1]*

Infectious Diseases Clinic, San Raffaele Scientific Institute, Milan, Italy[1]; Università degli Studi di Milano, Milan, Italy[2]; Istituto per lo Studio delle Macromolecole, CNR, Milan, Italy[3]; and Istituto di Chimica del Riconoscimento molecolare, CNR, Milan, Italy[4]

Received 15 October 2007/Accepted 28 January 2008

Antibodies to the first loop (ECL1) of CCR5 have been identified in human immunodeficiency virus (HIV)-exposed uninfected individuals (ESN) and in HIV-positive nonprogressing subjects. Thus, these antibodies may confer resistance against HIV infection. To define which amino acids are involved in antibody binding to CCR5, we performed a peptide-scanning assay and studied the immunogenicity of peptides in animal models. A panel of synthetic peptides spanning the CCR5-ECL1 region and displaying glycine or alanine substitutions was assayed for antibody binding with a pool of natural anti-CCR5 antibodies. We used mice and chickens to study the immunogenicity of mutagenized peptide. Structural characterization by nuclear magnetic resonance (NMR) spectroscopy and molecular dynamics simulations were performed to better understand the structural and conformational features of the mutagenized peptide. Amino acid substitutions in positions Ala95 and Ala96 (A_{95}-A_{96}) increased antibody-peptide binding compared to that of the wild-type peptide (Asp_{95}-Phe_{96}). The Ala95-96 peptide was shown to induce, in mice and chickens, antibodies displaying biological activity at very low concentrations. Strikingly, chicken antibodies to the Ala95-96 peptide specifically recognize human CCR5 molecules, downregulate receptors from lymphocytes, inhibit CCR5-dependent chemotaxis, and prevent infection by several R5 viruses, displaying 50% inhibitory concentrations of less than 3 ng/ml. NMR spectroscopy and molecular dynamics simulations proved the high flexibility of isolated epitopes and suggested that A_{95}-A_{96} substitutions determine a slightly higher tendency to generate helical conformations combined with a lower steric hindrance of the side chains in the peptides. These findings may be relevant to the induction of strong and efficient HIV-blocking antibodies.

The CCR5 coreceptor is a seven-transmembrane (TM)-spanning receptor involved in chemokine signaling (13, 35, 38). It also is used as a viral coreceptor by human immunodeficiency virus (HIV), and it presumably mediates the first contacts between HIV and target host cells in mucosal sites, as CCR5-tropic HIV strains are generally the first in pioneering new hosts (6, 8). The HIV-gp120 glycoprotein binds preferentially to the N terminus of CCR5 and the second extracellular region (18, 20). In addition, the second loop is mostly responsible for the binding of the endogenous chemokine peptides (42). Moreover, very recently a high level of immunogenicity has been found to both the N terminus and the first cysteine loop (49). Taken together, these findings suggest that the external domains of CCR5 are not clearly independent. In fact, it has been shown that CCR5 possesses a very dynamic equilibrium in the course of its interaction with Env proteins, which may induce different conformations in vivo (36). The binding of anti-gp120 immunoglobulins (Igs) also is known to alter the local conformation of viral and cellular proteins involved in the complex and therefore affect the whole process of HIV infection. (26).

Anti-CCR5 antibodies are a part of a peculiar immune response found specifically in a subset of exposed uninfected individuals (ESN) subjects distributed all over the world, including Caucasian and Asian subjects (2, 30, 31). They also have been found in a fraction of HIV-infected long-term nonprogressing subjects (37). Anti-CCR5 antibodies cause the internalization of CCR5 on membranes of $CD4^+$ T lymphocytes through a clathrin-dependent pathway, thus inducing a profound block to HIV infection (37). They also block viral translocation through epithelial cells by inducing CCR5 recruitment in the intracellular compartment, as reported previously (9).

Here, the amino acid sequence of the CCR5-ECL1 domain was analyzed by Ala/Gly mapping, with the aim of identifying amino acid positions essential to antigen-antibody binding and to assess the immunogenicity and the maintenance of biological properties of mutagenized antigen in two different animal models.

MATERIALS AND METHODS

Synthesis of peptides and preparation of peptide beads. Peptides were synthesized by the solid-phase Fmoc method (21) using an Applied Biosystems model 433 A peptide synthesizer. After peptide assembly, resin-bound peptides were deprotected as previously described (25) and purified to greater than 95% purity by semipreparative reverse-phase high-performance liquid chromatography (RP-HPLC). At the N and C termini, the peptides incorporated two additional glycines as spacers and two lysines to enable the covalent coupling of the

* Corresponding author. Mailing address: Infectious Diseases Clinic, San Raffaele Scientific Institute, Milan, Italy. Phone: 39-02-2643-7936. Fax: 39-02-2643-5381. E-mail: lopalco.lucia@hsr.it.

† Supplemental material for this article may be found at http://jvi.asm.org/.

▽ Published ahead of print on 6 February 2008.

TABLE 1. Constrained CCR5 peptides used in this study and amino acid sequences in ECL1 of CCR5 in the different species

Peptide	Sequence[a]
Human WT cyclic peptide	kgcYAAAQWDFGNTMCQgk
Gly 89	kgcG----------gk
Gly 90	kgc-G----------gk
Gly 91	kgc--G----------gk
Gly 92	kgc---G----------gk
Gly 93	kgc----G----------gk
Ala 94	kgc-----A--------gk
Ala 95	kgc------A-------gk
Ala 96	kgc-------A------gk
Ala 97	kgc--------A-----gk
Ala 98	kgc---------A----gk
Ala 99	kgc----------A---gk
Ala 100	kgc-----------A--gk
Ala 95-96	kgc------AA------gk
Human ECL1	YAAAQWDFGNTMCQ
Murine ECL 1	---NE-V---I--K
Chicken ECL 1	---HD-I-DALCR

[a] Small letters indicate extrasequence amino acids introduced to allow the etherocyclization of the peptides and to allow them to be coupled to Dynabeads.

peptides to Dynabeads. To obtain conformationally restricted, etherocyclic peptides, an extrasequence cysteine was added at the third position from the N terminus in each peptide. Oxidative folding was performed at neutral pH by overnight treatment at pH 7.4 (0.1 M Tris buffer) with a fivefold excess of oxidized glutathione, and the mixture was purified by RP-HPLC. The oxidative folding was monitored by analytical RP-HPLC; the folded oxidized monomeric peptide was eluted early from the column, while the reduced peptide and some polymeric material were eluted later. After the completion of the folding, the peptide solution was buffered to pH 2.2 with phosphoric acid, loaded into the semipreparative column, and purified from the polymeric material. The concentration of free sulfhydryl groups in the peptide from the semipreparative column was <0.1%, as checked by titration with Ellman's reagent (Pierce Biotechnology, Rockford, IL) (43).

Matrix-assisted laser desorption/ionization–time-of-flight mass spectrometry analysis of the alanine 95-alanine 96-folded peptide (designated Ala95-96) was 1,957.03 Da, in agreement with the expected value for the disulfide-bridged peptide (1,957.26 Da). The amino acid sequence of the peptide Ala95-96 was kgcYAAAQWAAGNTMCQck (extrasequence amino acids are in lowercase).

Peptide purity also was investigated by means of nuclear magnetic resonance (NMR) spectroscopy, which showed no additional NMR peaks caused by the short peptide fragment. Cyclization also was tested by measuring the presence of spatial connectivities among residues closely related to the cysteine residues.

The coupling of CCR5 or unrelated peptides (Table 1) to tosyl-activated M280 Dynabeads (Dynal, Oslo, Norway) was performed according to the manufacturer's instructions. Briefly, 3×10^7 beads were incubated with 9 μg of CCR5 peptides in 50 mM borate buffer, pH 9.5 (for 16 h at 37°C). After four washes in phosphate-buffered saline (PBS), peptide beads were ready to be used for human and mouse antibody screening. The binding of anti-CCR5-specific Igs to each peptide bead was obtained by incubating 9 μg immunoglobulin (Ig) with 9 μg peptide beads for 1 h at 4°C.

Mouse antibody generation and sample collection. Three groups of BALB/c mice were immunized with wild-type cyclic (cyclic WT), WT reduced (linear WT), and mutagenized cyclic (Ala95-96) peptides, each corresponding to the first cysteine loop of the extramembrane region of CCR5 (amino acids 89 to 100) (Table 1). In order to obtain a linear region, the WT peptide was not treated with glutathione. Mice were injected intraperitoneally with a solution of 10 μg of each immunogen in 200 μl of sterile PBS. Five immunizations were scheduled at weekly intervals. The first antigen dose was associated with Freund's complete adjuvant, the second injection was formulated in Freund's incomplete adjuvant, and subsequent immunizations did not include any adjuvant. Sera were collected weekly and pooled throughout the experiments. Anti-CCR5 responses were evaluated by enzyme-linked immunosorbent assay (ELISA) of the specific peptide. The institutional review board of the San Raffaele Scientific Institute, Milan, Italy, approved the investigations.

Chicken antibody generation and antibody recovery. Chickens were immunized subcutaneously with 0.1 mg of Ala95-96 per dose and 0.1 mg of cyclic WT peptides per dose, each covalently bound to keyhole limpet hemocyanin (Sigma-Aldrich, St. Louis, MO), at 3-week intervals. Antibody titers were measured in egg yolks 2 weeks after the third and fourth doses, on the free peptide as well as on ovalbumin-conjugated peptide, using an ELISA and horseradish peroxidase-conjugated rabbit anti-chicken IgY antibodies (Promega, Madison, WI) as the tracer. Each egg yolk was collected, brought to 25 ml with PBS, and, after the addition of 20 ml chloroform, was mixed and emulsified in a 50-ml Falcon tube. Centrifugation at $3,000 \times g$ was carried out at room temperature for 30 min. The upper liquid phase containing the proteins was collected and used for affinity purification on the Sepharose-bound peptide. The institutional review board of the University of Milan, Italy, approved the investigations.

Affinity purification of human and mouse antibodies and conjugation to peptide beads. Agarose beads, coupled with rabbit anti-human Ig or goat anti-mouse Ig (Sigma-Aldrich), were used to purify total Ig fractions from human sera and pre- and postimmune mouse sera. Ninety-six microliters of human sera or 60 μl of mouse sera was used, and Igs were obtained by elution with 0.2 M glycine-HCl buffer (pH 2); eluates were neutralized with 1 M Tris buffer, pH 11. The eluted Igs from human sera, immune mouse sera, and normal mouse sera (NMS) were dialyzed in PBS buffer and tested by ELISA using a standard procedure. The means of total Ig concentrations were 0.95 and 0.18 μg for human and mouse sera, respectively.

The binding of anti-CCR5-specific human Igs to peptide beads was obtained by incubating 9 μg of total Ig with 9 μg peptide beads for 1 h at 4°C. After being washed, Igs were eluted from the sample with 0.5 M acetic acid and dialyzed with RPMI medium. In brief, the specific CCR5 Igs from human or mouse sera were incubated for 1 h at 37°C on 96-microplate wells (Nunc, Roskilde, Denmark). Ig binding was evaluated by incubation with a 1:1,000 dilution of peroxidase-conjugated rabbit anti-human Ig (Dako Cytomation, Glostrup, Denmark) for 30 min at 37°C. The reaction was stopped and read at 492 nm with a microplate reader (Bio-Rad, Hercules, CA).

As the mean levels of human and mouse CCR5-specific antibodies were 0.5 and 30%, respectively, means of 0.045 and 2.7 μg of CCR5-specific antibodies, respectively, were obtained after a single round of purification.

Affinity purification of chicken antibodies and conjugation to peptide beads. The protein fraction was loaded on a 5-ml bed of a peptide-coupled Sepharose column and allowed to percolate by gravity under continuous absorbance monitoring. The column then was washed with PBS until the absorbance returned to baseline values. Glycine buffer (100 mM, pH 3.0) then was loaded, and the eluting peak was collected and immediately neutralized in 2 N NaOH. The chicken antibody was precipitated either with 16% (wt/vol) polyethylene glycol or with 50% (vol/vol) acetone, filtered, and stored at 4°C until use. CCR5-specific antibodies were obtained with the procedure described above for mouse antibodies. Chicken CCR5-specific antibody levels were 50% of the total amount of IgY, and a mean of 6 μg IgY was obtained after a single round of purification.

CCR5-specific antibody titer by ELISA. Fifty nanograms of free peptide was bound to the solid phase in carbonate-bicarbonate buffer (50 mM, pH 9.4) for 1 h. Serial twofold dilutions of egg yolk starting from 1:1,000 in PBS-bovine serum albumin then were exposed to the solid phase and were incubated at 37°C for 45 min. The plates were washed with an automatic plate washer (Bio-Rad) and exposed to the tracer. Absorbance was read at 490 nm using a plate reader (Bio-Rad) after 15 min of exposure of the samples to chromogen substrate (*O*-phenylenediamine dihydrochloride-H_2O_2) and blocking of the reaction with 2 N H_2SO_4.

The specific human and mouse CCR5-specific Igs were incubated for 1 h at 37°C on 96-microplate wells (Nunc). The Ig binding was evaluated by incubation with a 1:1,000 dilution of peroxidase-conjugated rabbit anti-human Ig or rabbit anti-mouse Ig (Dako) for 30 min at 37°C. The reaction was stopped and read at 492 nm by a microplate reader (Bio-Rad).

CCR5 internalization assay and flow cytometric analysis. Human (not carrying CCR5-Δ32 alleles) and mouse $CD4^+$ T lymphocytes were purified from resting peripheral blood mononuclear cells (PBMC) by immune adsorption to anti-$CD4^+$ magnetic beads (Oxoid, Hampshire, United Kingdom). Purified $CD4^+$ cells were stimulated with recombinant interleukin-2 (IL-2) or IL-12 (for mouse PBMC) (100 U/ml; Amersham, Buckinghamshire, United Kingdom), and then 10^5 cells were incubated with affinity-purified anti-CCR5 Ig (directed to ECL1) at 37°C for 48 h (to obtain a complete downregulation). Then 0.3 μg 2D7, a monoclonal antibody directed against the second loop (ECL2) of human CCR5, or 0.5 μg 45502.111 (a monoclonal antibody directed against the CCR5 N terminus) and 1 μg M20, a goat anti-mouse CCR5 antibody (Santa Cruz, Santa Cruz, CA), was incubated on 10^5 human or mouse $CD4^+$ lymphocytes. A control medium, containing 40 ng Igs from pooled sera of five untreated mice (NMS), was tested. A specific isotype control also was included (BD Bioscience Pharmingen, San Diego, CA). In order to verify the CCR5 internalization, cells also

were incubated with 50 nM RANTES for 1 h and then processed as described above. No evidence of CCR5 expression on the surface of CCR5-negative cell lines was seen. 2D7 was supplied by the AIDS Research and Reference Reagent Program. The relative percentage of CCR5 surface expression was calculated by measuring the mean channel fluorescence (MCF) according to the following equation: $100 \times [(MCF_{stimulated} - MCF_{negative\ control})/(MCF_{medium} - MCF_{negative\ control})]$. In some assays, 2×10^5 CCR5-transfected U87 cells were incubated with mouse/chicken antibodies to CCR5 (diluted 1:50) for 1 h at 4°C. Cells then were incubated with 2 μl of rabbit anti-mouse total Ig-FITC (Dako) or 2 μl of goat anti-chicken IgY-fluorescein isothiocyanate (FITC) (Santa Cruz) and with 5 μl of 2D7-phycoerythrin (PE) (BD Bioscience Pharmingen, San Diego, CA) for 30 min at 4°C. The latter assay was set up to verify that 2D7 incubation did not interfere with the binding of the chicken and mouse anti-CCR5 antibodies.

Chemotaxis. Human PBMC from one healthy donor were activated with phytohemagglutinin (PHA) and IL-2 for 3 days. A volume of 3×10^5 activated PBMC in 50 μl of RPMI 1640 medium containing 0.3% human serum albumin then was placed in the upper chamber of a 5-μm-pore-size bare-filter transwell (Costar Europe, Amsterdam, The Netherlands) and incubated with two concentrations of mouse affinity-purified anti-CCR5 Igs (28 and 2.8 ng/ml). A control medium containing 20 ng pooled total Igs from five untreated mice and 10% fetal calf serum (FCS) also was tested. Chemotaxis was conducted in the presence of 1.5 μg/ml of MIP-1β (placed in the lower chamber). The transwells were incubated for 2 h at 37°C; cells that migrated from the upper to the lower chamber then were quantified by fluorescence-activated cell sorter analysis. The results are expressed as the chemotaxis index, which represents the increase (*n*-fold) in the number of migrated cells in response to MIP-1β above that of spontaneous cell migration in control medium. The chemotaxis assay was repeated with PBMC from three different healthy donors (selected for high levels of CCR5 expression). All assays were performed in triplicate.

Virus isolation and titration. Subtype B viruses (HIV #36 and #40) were obtained as previously described (12, 28). In brief, HIV type 1 (HIV-1) was isolated from the PBMC of HIV-1-seropositive individuals by their cocultivation with PHA-stimulated PBMC of two healthy donors; the cultures were maintained until increasing levels of HIV-1–p24 antigen (Aalto Bio Reagents Ltd., Dublin, Ireland) were detected in two consecutive determinations. The 50% infective dose (ID_{50}) of each virus isolate was determined on PBMC from a single donor as follows. Six replicas (150 μl) of fivefold serial dilutions (from 1:5 to 1:3,125) of virus were added to 96 wells of a round-bottom microtiter plate (Nunc) containing 10^5 resting PBMC in 75 μl of medium and then were incubated at 37°C for 2 h. Medium then was removed, and fresh RPMI 1640 medium containing PHA (1 μg/ml) and recombinant IL-2 (10 U/ml) was added. The ID_{50} titers were defined as the reciprocal of the virus dilution yielding 50% positive wells by a Reed-Muench calculation.

Virus neutralization assays. The neutralizing activity was evaluated by two different methods. In the first method, SOS pseudoviruses were used to infect a CCR5-transfected U87 cell line as previously reported (7). Briefly, the plasmid pCAGGS was used to express membrane-bound Env of the R5 isolate JRFL. The plasmid pNL4-3.Luc.R-E-, expressing an HIV-1 genome fragment with frameshifts in Env and Vpr and a luciferase reporter gene in place of Nef (7), also was utilized. Pseudoviruses were produced by the transfection of 293T cells with pNL4-3.Luc.R-E- and Env-expressing pCAGGS-based plasmids. As a negative control, vesicular stomatitis virus G (VSV-G) pseudovirus was used. U87.CD4.CCR5 cells (10^4/well) were incubated with antibodies. After 48 h of incubation (to obtain a complete CCR5 downregulation), cultures were washed and SOS pseudoviruses (HIV-R5 and VSV-G) were incubated with cells for 2 h. Cells then were cultured for an additional 48 h, and the luciferase activity was measured by a previously reported method (14). The reaction was read by use of a Top Count apparatus (Packard, Meriden, CT). Each value obtained with a specific Ig dilution was compared to the mean value from the corresponding replicates without the addition of Igs, and HIV-blocking activity was expressed as the percentage of Ig concentrations leading to the blocking of viral replication.

In the second method, 2×10^5 resting PBMC were added to 75 μl of serial dilutions of chicken purified Ig to Ala95-96 peptide or chicken Ig to human Ig as a negative control. As positive controls, 30 μg/ml 2D7 (anti-CCR5 antibody) and serial dilutions of SIM4 (anti-CD4 antibody) were included. After 48 h of incubation (required to obtain a complete CCR5 downregulation) (3, 37), 75 μl of a virus dilution corresponding to 20 50% tissue culture IDs ($TCID_{50}$) was added. The cultures were incubated for an additional 2 h, washed, and resuspended in PHA- and IL-2-containing medium. Supernatant p24 levels were determined on days 5, 7, and 9 postinfection, and the analysis was performed when $TCID_{50}$s ranging from 10 to 30 were achieved. Since only small serum samples could be collected, the antibodies for the neutralization assay were purified from a pool of samples drawn after the fifth and sixth immunizations. Each dilution was tested in duplicate at virus concentrations ranging from 10 to 30 $TCID_{50}$; each experiment was repeated by using fresh PBMC from three different healthy blood donors. Each value obtained with a specific serum/Ig dilution was compared to the mean values from the six corresponding replicates without the addition of sera or Igs. Virus titration was repeated in each neutralization assay. The optical densities (ODs) in the replicates lacking the addition of sera ranged from 1.2 to 1.4 and corresponded to 100% viral replication. Thus, all of the results were expressed as percentages of antibody concentrations leading to the blocking of viral replication.

NMR solution structure determination. Peptide samples were obtained by dissolving WT and CCR5 etherocyclic peptides in H_2O-D_2O (90:10) solutions. The peptide concentration was ca. 4 mg in 500 μl of solvent for all samples. ^1H spectra were acquired at 11.7 T on a Bruker Avance DMX spectrometer equipped with a triple resonance *z* gradient probe with a proton frequency of 500.13 MHz. Time-proportional phase incrementation (32) was used to achieve quadrature detection in both dimensions. Solvent suppression was achieved by including the WATERGATE module (39) in the original two-dimensional total correlated spectroscopy (TOCSY) and nuclear Overhauser effect spectroscopy (NOESY) pulse sequences. Mixing times for TOCSY and NOESY spectra were 90 and 300 ms, respectively. All of the spectra were analyzed on an SGI Octane workstation equipped with the MSI Felix package.

Resonance assignments were performed by means of standard assignment procedures achieved via NOESY and TOCSY connectivities (19, 48). The volume of the assigned NOE cross-peaks from the NOESY spectra was measured by using the standard Felix integration routines and was converted into distances (1). Parameters used for structure calculations were described elsewhere (15).

Molecular dynamics (MD) simulations. For each etherocyclic peptide, the four most representative structures from a cluster analysis of the NMR structures were selected as the starting points for the four simulations. The cluster analysis on the NMR pool of structures was performed using the Gromos method (16). The number of neighbors of one structure was counted by using a cutoff based on a root mean squared deviation (RMSD) of 0.3 nm, and then the structure with the largest number of neighbors was taken, together with all of its neighbors, as a cluster and was eliminated from the pool of clusters. All of the MD runs and the analysis of the trajectories were performed using the GROMACS software package (version 3.2.1) (44). Charged terminal groups were used for each peptide, lysine amino acids were considered protonated, and the total charge of the peptides was +2. Each peptide was solvated with water in a periodic truncated octahedron large enough to contain the peptide and 0.8 nm of solvent on all sides. All solvent molecules within 0.15 nm of any peptide atom were removed. The simple point charge water model was used (4).

The simulations were performed at 300 K, and the temperature was maintained close to the intended value by weak coupling to an external temperature bath (5) with a coupling constant of 0.05 ps. The peptide and the solvent were coupled separately to the temperature bath. The GROMOS96 force field was used (45).

For water molecules, the SETTLE algorithm was used (34). A dielectric permittivity of $e = 1$ and a time step of 2 fs were used. The cutoffs were the same as those used for the GROMOS96 force-field parameterization (45). All of the simulations were equilibrated by a 50-ps MD run with position restraints on all protein atoms.

Four 20-ns MD simulations then were performed on each peptide in NTV conditions, where N is number of particles, T is temperature, and V is volume. Cluster analysis was performed on the resulting trajectories to define the most representative conformations accessible to the peptide. The Gromos method was applied to the trajectories (16). The secondary structure of each structure of the trajectories was classified by using the STRIDE dictionary (22). Graphical molecular models were generated by using the PyMOL software package (17).

Statistical analysis. Fisher's exact test was used to compare the mouse and chicken antibodies to each other.

RESULTS

Epitope mapping by an Ala/Gly-scanning peptide. Anti-CCR5 antibodies from ESN individuals previously were shown to specifically recognize ECL1 of the CCR5 coreceptor (31). In order to define which amino acids are involved in antibody binding to CCR5, a peptide-scanning experiment was performed. A pool of nine sera from ESN individuals previously shown to be positive for anti-CCR5 antibodies (9) was included in this study. These sera had antibodies that recognized

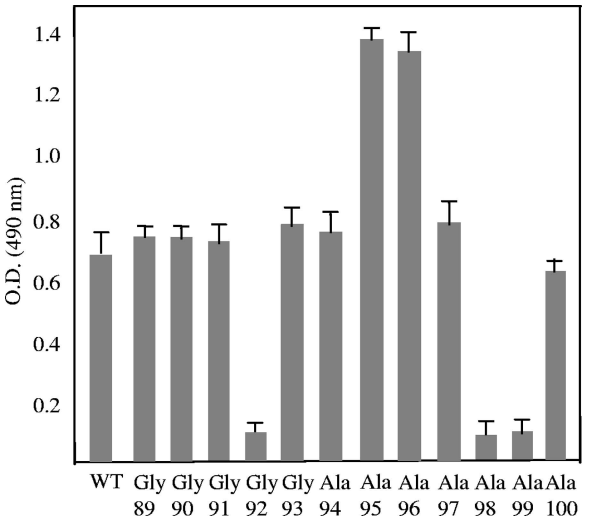

FIG. 1. Binding of human sera to mutagenized peptides covering the first external loop of CCR5. A panel of synthetic CCR5 loop 1 peptides, displaying glycine or alanine substitutions in positions 89 to 100, was assayed for antibody binding with a pool of anti-CCR5 antibodies from ESN individuals and compared to the antibody binding of the cyclic WT peptide (amino acids 89 to 100). Results represent the means from six replicate binding experiments; the top bars account for experimental variability.

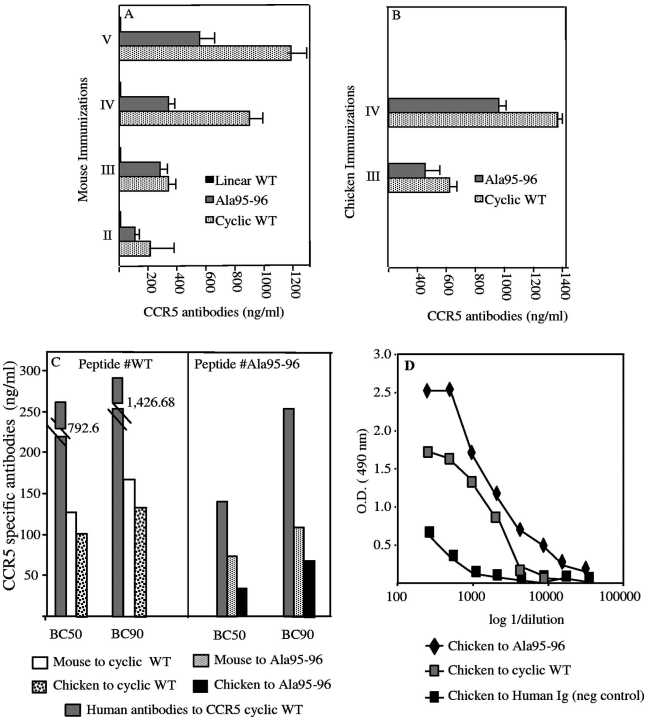

FIG. 2. Anti-CCR5 antibody titers induced in mice and chickens. (A) Mouse antiserum to Ala95-96 peptide in the cyclic conformation, its WT cyclic counterpart, and the native peptide in a linear conformation were analyzed by ELISA as described in Materials and Methods after the second, third, fourth, and fifth immunizations. Results show mean concentrations (in nanograms/milliliter) obtained in two assays performed; the top bars account for experimental variability. (B) Chickens were immunized with cyclic WT and Ala95-96 peptides at 3-week intervals. IgY antibodies were detected after the third and fourth immunizations by following the schedule presented in Materials and Methods. Chicken antibodies were tested at two concentrations (28 and 2.8 ng/ml). Results show mean values from two assays performed; the top bars account for experimental variability. (C) Human, mouse, and chicken CCR5-specific antibodies were quantified. Mouse antisera to cyclic WT and Ala95-96 peptides were tested after five immunizations. Chicken antibodies to cyclic WT and Ala95-96 peptides were tested after four immunizations. A pool of human sera from previously described (9) ESN having anti-CCR5 antibodies were tested for binding capacity on CCR5 cyclic WT and Ala95-96 peptides. Results are representative of the three assays performed. (D) Titration of anti-CCR5 chicken antibodies by ELISA as described in Materials and Methods. Chicken anti-human Ig was used as a negative control. Chicken antibodies were affinity purified as described in Materials and Methods and then quantified by ELISA. Chicken serum antibodies to Ala95-96 and to cyclic WT peptides were tested after four immunizations. Results are representative of the two independent assays performed.

a conformational epitope within CCR5-ECL1, and they induced a stable and long-lasting downregulation of CCR5 on the surface of T lymphocytes, which inhibit HIV entry (9).

A panel of synthetic CCR5-ECL1 peptides, displaying glycine or alanine punctual substitutions in the region of amino acids 89 to 100, was assayed for antibody binding with the pool of anti-CCR5 antibodies and compared to the binding of the WT peptide, as shown in Table 1. All peptides coupled to beads were assayed in native, cyclic structures, because the linear peptide previously was shown to be nonreactive in immune assays (31).

Effects induced by substitutions were divided into noninfluent, loss-of-function, and gain-of-function groups on the basis of their reactivity compared to that of the WT peptide reactivity. Peptides carrying amino acid changes in positions Gly92, Ala98, and Ala99 showed a sixfold lower reactivity than the WT peptide. Conversely, amino acid substitutions in positions Ala95 and Ala96 resulted in twofold increases in antibody-peptide binding, as shown in Fig. 1. Similar results were obtained when the double mutant Ala95-96 peptide was examined by ELISA; in particular, a mean optical density (OD) of 1.53 (range, 1.48 to 1.67 in three different experiments) was obtained. Thus, a peptide containing Ala95-Ala96 substitutions instead of the natural Phe95-Asp96 sequence was used in the immunization protocol.

Peptide Ala95-96 induces high-titer anti-CCR5 antibodies in mice and chickens. Amino acid substitutions conferring gain-of-function properties to ECL1 of CCR5 were included in a synthetic cyclic peptide, named Ala95-96, with the aim of investigating the biological properties of the mutated CCR5 domain via immunization in mice and chickens. The chicken model was used with the aim of testing the feasibility of a simple, inexpensive system to produce large amounts of Igs in hen eggs. The amino acid sequences of the different species used with CCR5-ECL1 are shown in Table 1.

The immunogenicity of either the CCR5 cyclic WT peptide or the mutagenized one (Ala95-96) was evaluated. Anti-CCR5-specific antibodies were detected in mouse sera from the second bleeding and reached a plateau after five immunizations, while the corresponding linear WT peptide, as expected and previously demonstrated (3), did not induce any response in mice (Fig. 2A). CCR5-specific antibodies in chickens were detected after three and four immunizations (Fig.

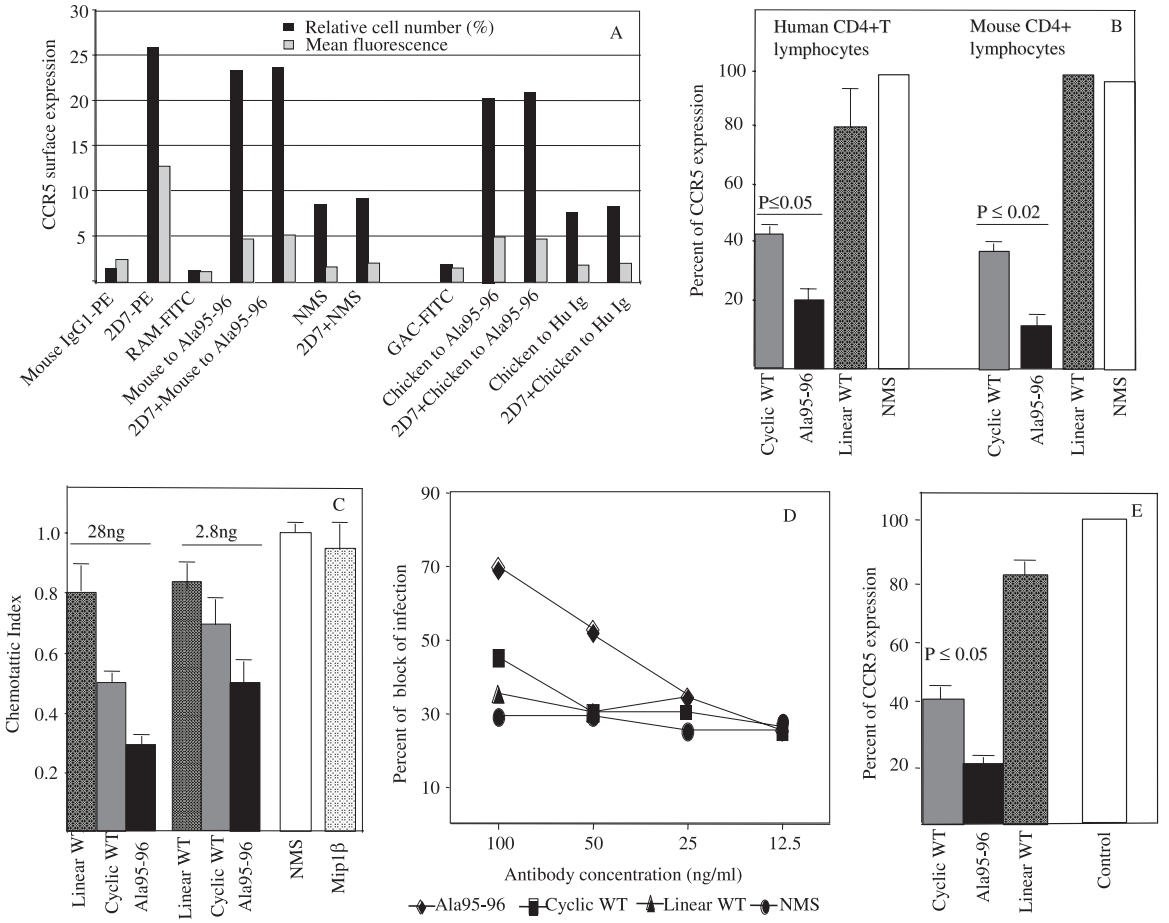

FIG. 3. Biological activity of immune responses elicited by the three different CCR5 peptides (cyclic WT, Ala95-95, and linear WT) in mice and chickens. (A) Flow cytometry analysis of the anti-CCR5 antibodies elicited in mice and chickens. CCR5 expression was evaluated by indirect binding of mouse and chicken antibodies in the presence or absence of 2D7 in human $CD4^+$ cells. The relative surface expression was evaluated either as the mean fluorescence or as a percentage of CCR5 expression. The isotype controls for 2D7 (mouse IgG1-PE), rabbit anti-mouse–FITC (RAM-FITC), goat anti-chicken–FITC (GAC-FITC), NMS, and chicken and human Igs were used as negative controls. 2D7 and the isotype control coupled to PE as well as RAM and GAC coupled to FITC were used. (B) CCR5 downregulation on human and mouse $CD4^+$ lymphocytes by 40 ng of CCR5-purified Ig from immunized mice. The CCR5 level was evaluated as the percentage of CCR5 expression by fluorescence-activated cell sorter analysis. Error bars represent standard deviations of three replicates for each data point. Assays were repeated three times with three different donors, and *P* values are shown. These data were obtained with serum samples drawn 1 week after the fifth immunization. (C) Inhibition of MIP-1β-induced chemotaxis of human $CD4^+$ lymphocytes by anti-CCR5 mouse antibodies. Purified lymphocytes were incubated with Ig fractions from antisera elicited by cyclic WT, Ala95-96, or linear WT peptide. Controls included lymphocytes treated with Ig fractions from NMS and those without added antibodies (FCS). The results are expressed as the mean of the chemotaxis index. Error bars represent standard deviations for three assays for each data point. (D) Dose-response curves of the blocking of the infectivity of an HIV-1 primary isolate (HIV #36, subtype B, R5-tropic virus) by anti-CCR5 mouse antibodies. As negative controls, serum-purified total Igs from a pool of five untreated mice (NMS) were used. The data are representative of the two experiments performed. (E) Antibody-mediated CCR5 downregulation in vivo. The CCR5 phenotype of $CD4^+$ lymphocytes was evaluated by flow cytometry of cells derived from peripheral blood of mice immunized with cyclic WT, Ala95-96, or linear WT peptide. The staining was obtained using M20 (anti-mouse polyclonal antibody). $CD4^+$ lymphocytes from untreated mice were used as positive controls for CCR5 expression. The data are expressed as the percentage of CCR5 expression and are shown as the averages from at least three independent experiments. *P* values also are shown.

2B). In both animal models, Ala95-96 peptide resulted in less immunogenicity than the cyclic WT peptide (Fig. 2A and B).

CCR5-specific antibodies were examined for their binding strengths to the CCR5 receptor. Mouse and chicken antibodies were tested on cyclic WT peptide. Anti-WT antibodies raised in chickens bound to the WT peptide more efficiently than the corresponding ones raised in mice, as shown by their 50 and 90% binding capacities (BC_{50} and BC_{90}, respectively) (Fig. 2C, left). Ala95-96 peptides induced better binding of specific antibodies in both the mouse and chicken models than that induced by cyclic WT peptide (Fig. 2C). Similar results were obtained with mouse total Ig and IgG fractions, thus confirming that Ala95-96 peptide induced antibodies that bind the CCR receptor more efficiently (data not shown). In addition, antibodies to Ala95-96 raised in chickens showed a higher binding efficiency than those in the corresponding mouse sera (Fig. 2C, right). These results were evident in both BC_{50} and BC_{90} assays, while human antibodies to cyclic WT and Ala95-96 peptides showed very low reactivities in both BC assays (Fig. 2C). Anti-CCR5 chicken antibodies were able to

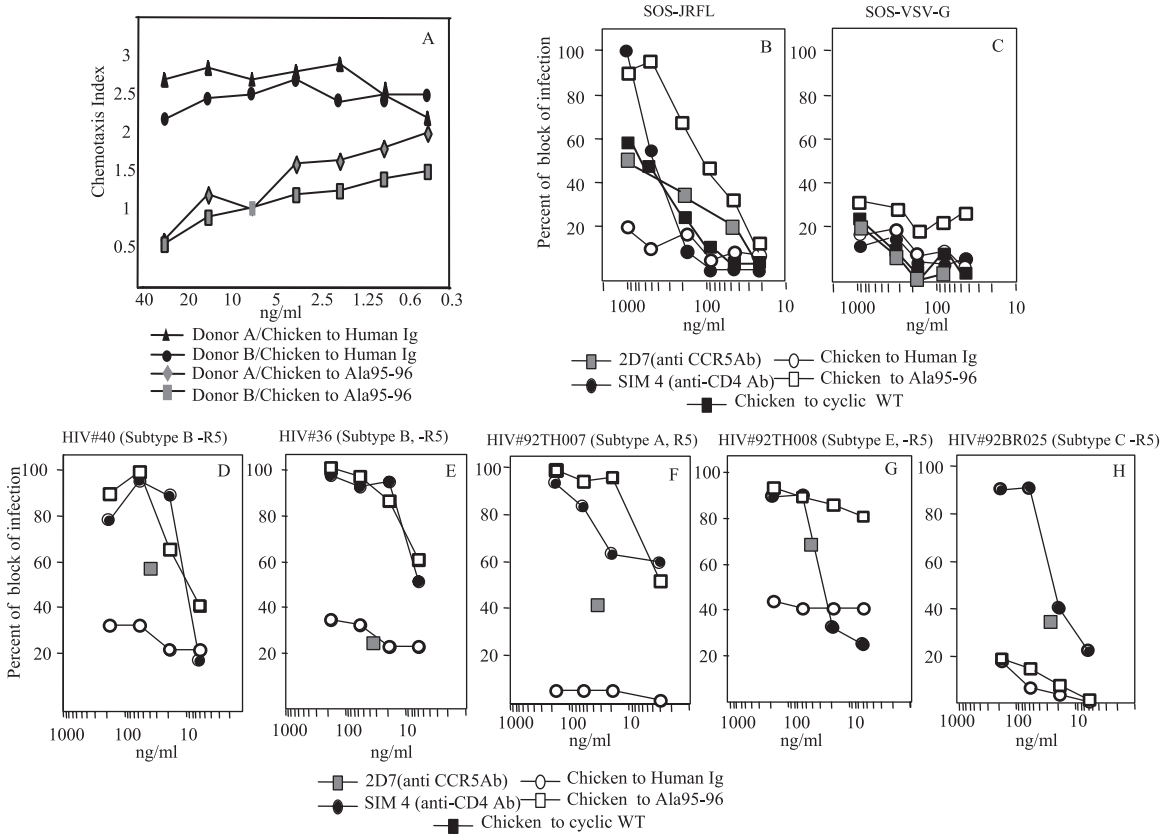

FIG. 4. Characterization of chicken immune responses elicited by Ala95-96 peptide. (A) Inhibition of MIP-1β-induced chemotaxis of human $CD4^+$ lymphocytes by anti-CCR5 chicken antibodies. Purified lymphocytes were incubated with chicken CCR5-specific IgY antibodies at concentrations ranging from 0.45 to 30 ng/ml. Lymphocytes from two healthy blood donors were used. Negative control included lymphocytes treated with IgY fractions from chicken antibodies to human Ig. Data are representative of the three assays performed. (B to H) Dose-response curves of the neutralization of the infectivity of HIV-1 strains by anti-CCR5 chicken antibodies. (B and C) Neutralization curves of SOS pseudoviruses JRFL and VSV. IgY fractions of the WT and Ala95-96 peptides were employed. As positive controls, SIM4 (anti-CD4 neutralizing monoclonal antibody) and 2D7 (anti-CCR5 neutralizing monoclonal antibody, tested at 30 μg/ml only) were used. As a negative control, IgY fractions of human Ig were tested. (D to H) HIV inhibition curves of a number of HIV-1 primary isolates. Primary isolates HIV #40 and #36 were subtype B and R5 tropic. HIV #92TH007, #92TH008, and #92BR025 were subtypes A, E, and C, respectively, and were R5 tropic, and they were provided by the AIDS Reference Research and Reagent Program. Antibodies were tested from 6 to 200 ng/ml. 2D7 (at 30 μg) and SIM4 were used as positive controls, and a chicken antibody to human Ig was used as a negative control. All data are representative of at least three of the independent assays performed.

bind Ala95-96 peptide in an ELISA at dilutions ranging from 1:50 to 1:20,000 (Fig. 2D). A very small amount of chicken antibody is needed to bind 50 and 90% of peptide (37 and 72 ng/ml, respectively), thus indicating that the chicken model elicited the antibodies that bound most efficiently to the mutagenized peptide of CCR5 (Fig. 2C, right). To confirm these results, a pool of mice antisera (drawn 1 week after the last immunization) was screened at a 1:100 dilution with glycine, and it gave negative results (mean ODs, 0.107 and 0.075 for mouse antisera to Ala95-96 and cyclic WT peptides, respectively), while chicken anti-Ala95-96 antibodies showed a mean OD of 0.300 when screened with glycine.

Peptide Ala95-96 induces stronger in vitro and ex vivo anti-CCR5 biologic activities than cyclic WT peptide in mice and chickens. We previously demonstrated that anti-CCR5 Ig found in humans induced a long-lasting downregulation of the receptor in a clathrin-dependent pathway, which blocked HIV entry (9, 30, 37). In addition, mouse antibodies to CCR5-ECL1 induced the internalization of CCR5 with kinetics similar to that observed with human antibodies to ECL1 of CCR5, as previously reported (3). Briefly, CCR5 downregulation on target cells was achieved after 48 h of treatment with CCR5-specific Igs (either in humans or in mice), whereas an intermediate value was obtained after 24 h of incubation (data not shown) (9, 30, 37). Moreover, as previously demonstrated, CCR5 modulation was not evident after 1 h of anti-CCR5-ECL1 antibody incubation (9, 30, 37), thus demonstrating that mouse and chicken antibodies do not interfere with the binding of 2D7 or 45502.111 (directed to ECL2 and the N terminus, respectively) on the surfaces of $CD4^+$ cells. In addition, the incubation with 2D7 or 45502.111 did not interfere with mice or chicken antibody binding activity on the CCR5-transfected U87 cell line (Fig. 3A). Thus, anti-CCR5 antibodies raised to peptides were assayed for biological activity with the CCR5 coreceptor after 48 h of incubation of anti-CCR5 antibodies. Anti-CCR5 antibodies from Ala95-96 peptide-immunized mice downregulated CCR5 molecules on $CD4^+$ T lymphocytes from healthy human donors and murine $CD4^+$ peripheral lym-

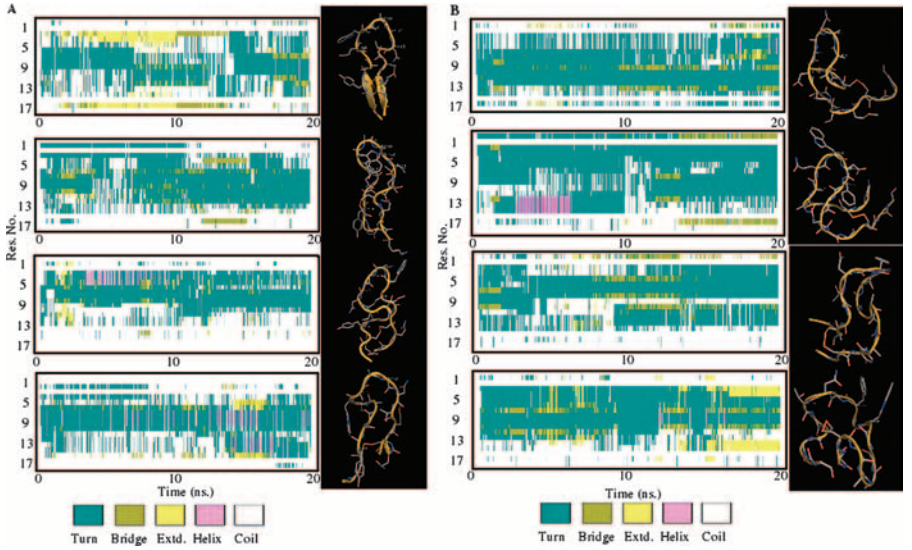

FIG. 5. Secondary structure and models of Ala95-96 and cyclic WT peptides. (A) Structure and model of the WT peptide. The left side shows the time evolution of the secondary structure of the WT peptide in each of the four MD simulations. For each frame of the trajectory, the algorithm STRIDE assigned the secondary structure of each residue of the peptide. Different secondary-structure motifs are identified by the color code depicted in the legend. The right side shows a representation of the most populated structure of the peptide extracted by the cluster analysis of each trajectory. (B) Structure and model of the Ala95-96 peptide. The left side shows the time evolution of the secondary structure of the peptide in each of the four MD simulations. For each frame of the trajectory, the algorithm STRIDE assigned the secondary structure of each residue of the peptide. Different secondary-structure motifs are identified by the color code depicted in the legend. The right side shows a representation of the most populated structure of the peptide extracted by the cluster analysis of each trajectory.

phocytes (Fig. 3B). Antibodies from mice immunized with WT cyclic peptide were less effective in downregulating surface CCR5 receptors in both assays (data not shown) (3). CCR5 downregulation induced by mouse antibodies to Ala95-96 was stronger than that induced by mouse antibodies to cyclic WT peptide, and the difference was statistically significant on human T lymphocytes ($P \leq 0.05$) and on mouse T lymphocytes ($P \leq 0.02$) (Fig. 3B). Moreover, the preincubation of 2D7 or 45502.111 on human $CD4^+$ T cells or the preincubation of M20 on mouse $CD4^+$ T cells did not interfere with mouse or chicken antibody binding activity (data not shown).

Similarly, Igs from Ala95-96 peptide-immunized mice were more effective in inhibiting MIP-1β-induced chemotaxis than cyclic WT peptide (Fig. 3C). Igs induced by linear WT peptide had a poor effect both on human $CD4^+$ cells and in the chemotactic assay and also were unable to downregulate CCR5 receptors on murine $CD4^+$ lymphocytes (Fig. 3B and C).

We verified whether mouse CCR5-specific sera also could block HIV infectivity. As the 50% inhibitory concentration (the serum dilution blocking 50% of viral replication) of antisera to Ala95-96 peptide was achieved at 1:80, serum affinity-purified total Igs from mice immunized with the different peptides (cyclic WT, linear WT, and Ala95-96) also were tested (Fig. 3D). Mouse antibodies to Ala95-96 peptide were able to specifically block the infectivity of HIV #36 (a B-subtype primary isolate). Quiescent PBMC were used in the HIV-blocking assay. Cells were activated at the time of infection. In these conditions, the low level of CCR5 surface expression is appropriated to set up a CCR5-dependent HIV-blocking assay (31, 37). Mouse antisera to linear WT or to cyclic WT peptide did not affect HIV infectivity (Fig. 3D), as expected and previously reported (3).

The effect of anti-CCR5 antibodies on downregulating surface CCR5 molecules also was analyzed. $CD4^+$ cells were isolated from murine PBMC collected after the fifth immunization. The level of CCR5 downregulation was higher in mice immunized with Ala95-96 peptide than in mice treated with cyclic WT peptide, and the difference was statistically significant ($P \leq 0.05$) (Fig. 3E). Antibodies raised to linear WT peptide slightly affected CCR5 downregulation and chemotaxis with respect to control pooled sera (NMS).

Biological properties of anti-CCR5 antibodies raised in chickens with Ala95-96 peptide also were tested. CCR5-specific chicken Igs were able to inhibit specific chemotactic effects of MIP-1β on human $CD4^+$ lymphocytes from two different donors (Fig. 4A), while a chicken IgY to human Igs, assayed as a negative control, did not affect chemotaxis.

The HIV-blocking ability of anti-CCR5 chicken antibodies was confirmed by using two assays. Chicken antibodies to Ala95-96 peptide specifically blocked the infectivity of the JRFL strain in the SOS neutralization assay. A weaker activity was shown with chicken serum to WT peptide. Similar assays, performed with VSV-G virus, gave negative results (Fig. 4B and C).

Anti-Ala95-96 chicken antibodies also were tested on some R5 HIV primary isolates belonging to subtypes A, B, C, and E (Fig. 4D to H). The experimental conditions were the same as those reported for the evaluation of the HIV-blocking activity of mouse antisera. Chicken antibodies blocked the infection of four out of five isolates assayed. Chicken antibodies inhibited the infectivity of some HIV isolates at concentrations even lower than those of the SIM4 monoclonal antibody used as a control (Fig. 4F, G).

NMR structural determination and MD simulations. Monodimensional proton NMR spectra acquired on both the cyclic WT peptide and the more active cyclic peptide Ala95-96 (Table 1) in water showed the amide proton couplings typical of the extended conformation (6 to 7 Hz), thus indicating no preferential conformation in solution. The α proton chemical shift indexes (47) were employed initially to explore the existence of a secondary structure different for the two cyclic peptides (WT and Ala95-96). These indexes derive mainly from local magnetic fields arising from the orientation of the peptide groups (Ψ and Φ angles) and therefore are related to the backbone conformation. As indicated in Fig. 5, a slight tendency to helical conformation for residues A6 to N13 is present.

The conformation family obtained, consisting of 50 structures, was fully consistent with the NMR constraints used, showing a backbone RMSD of 4 Å, thus confirming the absence of a preferential conformation.

We investigated the conformational dynamics of the two peptides at an atomically detailed level by means of MD simulations in an explicit solvent, starting from the four most representative structures that satisfy the NMR distance constraints of the cyclic WT and Ala95-96 peptides in solution. Four simulations of 20 ns each were started for each peptide in solution, for a total sampling of 80 ns for both cyclic WT and Ala95-96 peptides. The simulations showed extensive sampling of the conformational space around the NMR-determined structures and allowed us to address issues related to the conformational dynamics of the peptides in solution before molecular recognition by the receptor.

Figure 5 represents the time evolution of the secondary structure of the cyclic peptides isolated in solution, together with the three-dimensional structure of the most populated conformation in the respective trajectory, selected by the cluster analysis method described in Material and Methods. The molecules in these simulations nevertheless do sample a series of conformations basically characterized by the presence of bends and turns located along the central residues of the sequences (residues 4 to 15). It is worth noting that the MD simulations of the Ala95-96 mutant (Fig. 5B) show a helical propensity for residues 7 to 9, in agreement with the NMR data, in which the $d(d_{Ca})$ data point to the presence of a partial helical structure.

Cluster analysis of the structures from all of the simulations after the superposition of all C-α atoms gives a total of 24 different structural clusters for the Ala95-96 peptide and 12 for the cyclic WT peptide, with an average RMSD of 0.43 nm for the Ala95-96 peptide and 0.49 for the cyclic WT peptide. These results reflect once more the very flexible nature of the peptides.

Moreover, a chemical shift index was made, families of 50 conformers were determined by restrained MD, and TOCSY spectra were determined and are shown in the supplemental material (see Fig. S1, S2, and S3 in the supplemental material).

The peptide with the highest activity is the one in which a partially ordered helical secondary structure can form due to the high helical propensities of alanine residues (Ala95-96). This partial preorganization in the structure of the more active peptide, combined with the minimal steric hindrance characterizing alanine substitutions, may be a factor in the molecular recognition process with the receptor.

DISCUSSION

Epitope mapping performed with the first loop of the CCR5 protein showed five amino acid positions, 92, 95, 96, 98, and 99, that influence the affinities and biological properties of anti-CCR5 antibodies. The mutations N98A and T99A demonstrated the importance of hydrophilic residues in positions 98 and 99, while in positions 95 and 96, hydrophobic groups are required to increase the interaction with the Igs. Moreover, when positions 95 and 96 both are occupied by hydrophobic residues, the peptide shows a binding activity greater than that of other sequences we tested. Very recently it has been demonstrated by using peptide mimotopes that position 96 in ECL1 is one of the critical residues for HIV-1 entry (27a). The mutation A92G also showed that the presence of a hydrophobic residue in position 92 is determinant for the binding. Thus, the precise identification of cellular domains relevant to obtaining an efficient blocking of HIV entry into host cells should clarify the molecular basis of viral entry and facilitate the rational design of inhibitory molecules for therapy such as that using HIV-blocking antibodies.

When assayed as an immunogen in the mouse model, peptide Ala95-96 was able to induce lower antibody titers than those of the cyclic WT peptide of amino acids 89 to 100, but its antibodies showed a significantly higher binding capacity to CCR5 peptides than their counterparts induced by cyclic WT peptide. Anti-Ala95-96 Igs induced a stronger CCR5 downregulation on both murine and human $CD4^+$ lymphocytes than antibodies raised to cyclic WT peptide in both in vitro and ex vivo experiments. Moreover, anti-CCR5-modified peptide antibodies hampered chemotactic effects mediated by this receptor more effectively than antibodies raised to cyclic WT peptide. Anti-CCR5 antibodies induced by modified peptide were shown to be 10 times more effective than the monoclonal antibody-positive controls in HIV-blocking tests against different viral subtypes. Such findings could be relevant to the generation of a new class of HIV-blocking antibodies with better affinity to the receptor. Moreover, the mutagenized peptide Ala95-96 could be useful, at least in theory, to design new microbicides. As very recently reported, several classes of entry inhibitors, including peptides and antibodies to CCR5, are in preclinical evaluation or might be microbicide candidates (27).

Similar results were obtained from chicken experiments, thus confirming our findings in at least two different animal models. The avian animal model is a simple, inexpensive model; the production of large amounts of antibodies to be employed in further characterizations is feasible. Chicken antibodies were able to exert biologic effects on both human $CD4^+$ $CCR5^+$ cells as well as on endogenous receptors, and they blocked the HIV infection of different subtypes at very low concentrations (less than 3 ng/ml).

The availability of large amounts of antibodies that were raised in chickens at low cost could be useful in scientific research. Zhu et al. have recently demonstrated that chimeric chickens can secrete milligrams of fully human monoclonal antibodies with characteristics suitable for therapeutic use into their eggs. Thus, they demonstrated the potential for mono-

clonal antibody production in chicken eggs as a viable alternative to the traditional mammalian cell culture system (50).

Analyzing the profile of the sequences of the Ala/Gly mapping, the results of structural analysis, and the results of the immunological assays, it appears that the replacement of a hydrophilic amino acid, aspartic acid, in position 95 with a hydrophobic residue, alanine, and the presence of another hydrophobic residue in position 96 improves the immunological activity of the peptide with respect to that of the WT sequence. Structural analysis by NMR spectroscopy and MD simulations showed very high conformational flexibility for both the WT and the more active Ala95-96 peptide, confirming the well-known features of the mobility of the protein loop regions in general and of CCR5 in particular. Interestingly, MD and NMR data suggest a defined tendency to populate helical structures in the most active Ala95-96 peptide. The presence of this ordered secondary-structure motif may play a role in preorganizing the isolated peptide for the binding and recognition with its respective antibody. The different structural behavior of this loop may account for a better molecular structural organization, allowing the induction of the fittest antibodies, which recognize and bind native CCR5 with higher affinity and display enhanced biological activity. As the structure of CCR5 has not been determined and multiple ECLs of the receptor are claimed to be permissive for HIV entry, the definition of the structure of the specific CCR5 regions/peptides that are relevant for HIV entry is extremely relevant for the design of therapeutics, as has been reported for the N terminus of CCR5 (24).

Although the whole CCR5 structure has not been solved, the structure of the human β2-adrenergic receptor (β2AR) recently was solved by several collaborating research groups (11, 40, 41). These X-ray structures showed the overall folding of the receptor consisting of seven TM helices and the short loops connecting them. These extracellular loops may play a relevant role in the pharmacology of every receptor and in the structural stability of the protein itself. With the exception of the ECL2 described by Cherezov et al. (11), which consists of a short extrahelical segment reinforced by two disulfide bonds, the ECLs of β2ARs are poorly structured and show high flexibility (11, 40, 41). These findings are in good agreement with our results, thus suggesting that the structures of both CCR5 and β2AR are similar, at least for some ECLs, including ECL1.

Loop proteins often are endowed with multiple conformations that can mediate protein-protein interactions in ligand binding or in other biologic functions. In the case of a surface receptor, such as the CCR5 protein, changes in protein conformations are known to reflect different activation states (33). CCR5 dimerization was shown to block HIV infectivity via a chemokine-dependent mechanism (46). Strikingly, mutations involving the structure of the first external loop of CCR5 were shown to affect CCR5 function and HIV infectivity deeply. Changes in the second and the third CCR5 loop (TM3 and TM4) may affect the conformation of monomeric-only CCR5 mutants (10, 23). However, mutations occurring in CCR5 domains other than the second external loop, such as Δ32, may have a significant impact on the biological function of the receptor. As a consequence, new, highly immunogenic epitopes might be displayed in the course of this multiphased and complex process of virus-host interaction (29).

Moreover, the results of these experiments confirm that conformational changes in the CCR5 protein, together with host factors, may account for changes in protein immunogenicity in vivo and therefore are expected to play a role in the natural resistance to HIV infection.

ACKNOWLEDGMENTS

We thank S. Russo for editorial help.

This work was supported by Istituito Superiore di Sanita grants 45G18 and 40G34 to L.L.

REFERENCES

1. **Baleja, J. D., T. Mau, and G. Wagner.** 1994. Recognition of DNA by GAL4 in solution: use of a monomeric protein-DNA complex for study by NMR. Biochemistry **33:**3071–3078.
2. **Barassi, C., A. Lazzarin, and L. Lopalco.** 2004. CCR5-specific mucosal IgA in saliva and genital fluids of HIV-exposed seronegative subjects. Blood **104:**2205–2206.
3. **Barassi, C., E. Soprana, C. Pastori, R. Longhi, E. Buratti, F. Lillo, C. Marenzi, A. Lazzarin, A. G. Siccardi, and L. Lopalco.** 2005. Induction of murine mucosal CCR5-reactive antibodies as an anti-human immunodeficiency virus strategy. J. Virol. **79:**6848–6858.
4. **Berendsen, H. J. C., J. R. Grigera, and T. P. Straatsma.** 1987. The missing term in effective pair potentials. J. Phys. Chem. **91:**6269–6271.
5. **Berendsen, H. J. C., J. P. M. Postma, W. F. van Gunsteren, A. Di Nola, and J. R. Haak.** 1984. Molecular dynamics with coupling to an external bath. J. Chem. Phys. **81:**3684.
6. **Berger, E. A., P. M. Murphy, and J. M. Farber.** 1999. Chemokine receptors as HIV-1 coreceptors: roles in viral entry, tropism, and disease. Annu. Rev. Immunol. **17:**657–700.
7. **Binley, J. M., C. S. Cayanan, C. Wiley, N. Schulke, W. C. Olson, and D. R. Burton.** 2003. Redox-triggered infection by disulfide-shackled human immunodeficiency virus type 1 pseudovirions. J. Virol. **77:**5678–5684.
8. **Blaak, H., A. B. van't Wout, M. Brouwer, M. Cornelissen, N. A. Kootstra, N. Albrecht-van Lent, R. P. Keet, J. Goudsmit, R. A. Coutinho, and H. Schuitemaker.** 1998. Infectious cellular load in human immunodeficiency virus type 1 (HIV-1)-infected individuals and susceptibility of peripheral blood mononuclear cells from their exposed partners to non-syncytium-inducing HIV-1 as major determinants for HIV-1 transmission in homosexual couples. J. Virol. **72:**218–224.
9. **Bomsel, M., C. Pastori, D. Tudor, C. Alberti, S. Garcia, D. Ferrari, A. Lazzarin, and L. Lopalco.** 2007. Natural mucosal antibodies reactive with first extracellular loop of CCR5 inhibit HIV-1 transport across human epithelial cells. AIDS **21:**13–22.
10. **Chelli, M., and M. Alizon.** 2001. Determinants of the trans-dominant negative effect of truncated forms of the CCR5 chemokine receptor. J. Biol. Chem. **276:**46975–46982.
11. **Cherezov, V., D. M. Rosenbaum, M. A. Hanson, S. G. F. Rasmussen, F. S. Thian, T. S. Kobilka, H. Choi, P. Kuhn, W. I. Weis, B. K. Kobilka, and R. C. Stevens.** 2007. High resolution crystal structure of an engineered human β2 adrenergic G protein-coupled receptor. Science **318:**1258–1265.
12. **Clerici, M., C. Barassi, C. Devito, C. Pastori, S. Piconi, D. Trabattoni, R. Longhi, J. Hinkula, K. Broliden, and L. Lopalco.** 2002. Serum IgA of HIV-exposed uninfected individuals inhibit HIV through recognition of a region within the alpha-helix of gp41. AIDS **16:**1731–1741.
13. **Cohen, J.** 1997. Exploiting the HIV-chemokine nexus. Science **275:**1261–1264.
14. **Connor, R. I., B. K. Chen, S. Choe, and N. R. Landau.** 1995. Vpr is required for efficient replication of human immunodeficiency virus type-1 in mononuclear phagocytes. Virology **206:**935–944.
15. **Consonni, R., L. Santomo, P. Fusi, P. Tortora, and L. Zetta.** 1999. A single-point mutation in the extreme heat- and pressure-resistant sso7d protein from Sulfolobus solfataricus leads to a major rearrangement of the hydrophobic core. Biochemistry **38:**12709–12717.
16. **Daura, X., K. Gademann, B. Jaun, D. Seebach, W. F. van Gunsteren, and A. E. Mark.** 1999. Peptide folding: when simulation meets experiment. Angew. Chemie Intl. **38:**236–240.
17. **DeLano, W. L.** 2002. The PyMOL molecular graphics system. DeLano Scientific, San Carlos, CA.
18. **Dragic, T., A. Trkola, S. W. Lin, K. A. Nagashima, F. Kajumo, L. Zhao, W. C. Olson, L. Wu, C. R. Mackay, G. P. Allaway, T. P. Sakmar, J. P. Moore, and P. J. Maddon.** 1998. Amino-terminal substitutions in the CCR5 coreceptor impair gp120 binding and human immunodeficiency virus type 1 entry. J. Virol. **72:**279–285.
19. **Englander, S. W., and A. J. Wand.** 1987. Main-chain-directed strategy for the assignment of ^{1}H NMR spectra of proteins. Biochemistry **26:**5953–5958.
20. **Farzan, M., H. Choe, L. Vaca, K. Martin, Y. Sun, E. Desjardins, N. Ruffing, L. Wu, R. Wyatt, N. Gerard, C. Gerard, and J. Sodroski.** 1998. A tyrosine-

rich region in the N terminus of CCR5 is important for human immunodeficiency virus type 1 entry and mediates an association between gp120 and CCR5. J. Virol. **72:**1160–1164.
21. **Fields, G. B., and R. L. Noble.** 1990. Solid phase peptide synthesis utilizing 9-fluorenylmethoxycarbonyl amino acids. Int. J. Pept. Protein Res. **35:**161–214.
22. **Frishman, D., and P. Argos.** 1995. Knowledge-based protein secondary structure assignment. Proteins **23:**566–579.
23. **Hernanz-Falcón, P., J. M. Rodriguez-Frade, A. Serrano, D. Juan, A. del Sol, S. F. Soriano, F. Roncal, L. Gomez, A. Valencia, A. C. Martinez, and M. Mellado.** 2004. Identification of amino acid residues crucial for chemokine receptor dimerization. Nat. Immunol. **5:**216–223.
24. **Huang, C. C., S. N. Lam, P. Acharya, M. Tang, S. H. Xiang, S. S. Hussan, R. L. Stanfield, J. Robinson, J. Sodroski, I. A. Wilson, R. Wyatt, C. A. Bewley, and P. D. Kwong.** 2007. Structures of the CCR5 N terminus and of a tyrosine-sulfated antibody with HIV-1 gp120 and CD4. Science **317:**1930–1934.
25. **King, D. S., C. G. Fields, and G. B. Fields.** 1990. A cleavage method which minimizes side reactions following Fmoc solid phase peptide synthesis. Int. J. Pept. Protein Res. **36:**255–266.
26. **Klasse, P. J., and Q. J. Sattentau.** 2002. Occupancy and mechanism in antibody-mediated neutralization of animal viruses. J. Gen. Virol. **83:**2091–2108.
27. **Klasse, P. J., R. Shattock, and J. P. Moore.** 2008. Antiretroviral drug-based microbicides to prevent HIV-1 sexual transmission. Annu. Rev. Med. **59:**291–307.
27a. **Konigs, C., A. Pustowka, J. Irving, C. Kessel, K. Klich, V. Wegner, M. J. Rowley, I. R. Mackay, W. Kreuz, C. Griesinger, and U. Dietrich.** 2007. Peptide mimotopes selected with HIV-1-blocking monoclonal antibodies against CCR5 represent motifs specific for HIV-1 entry. Immunol. Cell Biol. **85:**511–517.
28. **Lisziewicz, J., E. Rosenberg, J. Lieberman, H. Jessen, L. Lopalco, R. Siliciano, B. Walker, and F. Lori.** 1999. Control of HIV despite the discontinuation of antiretroviral therapy. N. Engl. J. Med. **340:**1683–1684.
29. **Lopalco, L.** 2004. Humoral immunity in HIV-1 exposure: cause or effect of HIV resistance? Curr. HIV Res. **2:**127–139.
30. **Lopalco, L., C. Barassi, C. Paolucci, D. Breda, D. Brunelli, M. Nguyen, J. Nouhin, T. T. Luong, L. X. Truong, M. Clerici, G. Calori, A. Lazzarin, G. Pancino, and S. E. Burastero.** 2005. Predictive value of anti-cell and anti-human immunodeficiency virus (HIV) humoral responses in HIV-1-exposed seronegative cohorts of European and Asian origin. J. Gen. Virol. **86:**339–348.
31. **Lopalco, L., C. Barassi, C. Pastori, R. Longhi, S. E. Burastero, G. Tambussi, F. Mazzotta, A. Lazzarin, M. Clerici, and A. G. Siccardi.** 2000. CCR5-reactive antibodies in seronegative partners of HIV-seropositive individuals down-modulate surface CCR5 in vivo and neutralize the infectivity of R5 strains of HIV-1 in vitro. J. Immunol. **164:**3426–3433.
32. **Marion, D., and K. Wuthrich.** 1983. Application of phase sensitive two-dimensional correlated spectroscopy (COSY) for measurements of 1H–1H spin-spin coupling constants in proteins. Biochem. Biophys. Res. Commun. **113:**967–974.
33. **Mellado, M., J. M. Rodriguez-Frade, S. Manes, and A. C. Martinez.** 2001. Chemokine signaling and functional responses: the role of receptor dimerization and TK pathway activation. Annu. Rev. Immunol. **19:**397–421.
34. **Miyamoto, S., and P. A. Kollman.** 1992. Settle: an analytical version of the shake and rattle algorithms for rigid water models. J. Comp. Chem. **13:**952–962.
35. **Moore, J. P.** 1997. Coreceptors: implications for HIV pathogenesis and therapy. Science **276:**51–52.
36. **Parren, P. W., M. C. Gauduin, R. A. Koup, P. Poignard, P. Fisicaro, D. R. Burton, and Q. J. Sattentau.** 1997. Relevance of the antibody response against human immunodeficiency virus type 1 envelope to vaccine design. Immunol. Lett. **57:**105–112.
37. **Pastori, C., B. Weiser, C. Barassi, C. Uberti-Foppa, S. Ghezzi, R. Longhi, G. Calori, H. Burger, K. Kemal, G. Poli, A. Lazzarin, and L. Lopalco.** 2006. Long-lasting CCR5 internalization by antibodies in a subset of long-term nonprogressors: a possible protective effect against disease progression. Blood **107:**4825–4833.
38. **Paterlini, M. G.** 2002. Structure modeling of the chemokine receptor CCR5: implications for ligand binding and selectivity. Biophys. J. **83:**3012–3031.
39. **Piotto, M., V. Saudek, and V. Sklenar.** 1992. Gradient-tailored excitation for single-quantum NMR spectroscopy of aqueous solutions. J. Biomol. NMR **2:**661–665.
40. **Rasmussen, S. G. F., H. Choi, D. M. Rosenbaum, T. S. Kobilka, F. S. Thian, P. C. Edwards, M. Burghammer, V. R. P. Ratnala, R. Sanishvili, R. F. Fischetti, G. F. X. Scheltler, W. I. Weis, and B. K. Kobilka.** 2007. Crystal structure of the human β2 adrenergic G-protein-coupled receptor. Nature **450:**383–388.
41. **Rosenbaum, D. M., V. Cherezov, M. A. Hanson, S. G. Rasmussen, F. S. Thian, T. S. Kobilka, H. J. Choi, X. J. Yao, W. I. Weis, R. C. Stevens, and B. K. Kobilka.** 2007. GPCR engineering yields high-resolution structural insights into β2-adrenergic receptor function. Science **318:**1266–1273.
42. **Samson, M., G. LaRosa, F. Libert, P. Paindavoine, M. Detheux, G. Vassart, and M. Parmentier.** 1997. The second extracellular loop of CCR5 is the major determinant of ligand specificity. J. Biol. Chem. **272:**24934–24941.
43. **Sedlak, J., and R. H. Lindsay.** 1968. Estimation of total, protein bound, and non-protein sulfhydryl groups in tissue with Ellman's reagent. Anal. Biochem. **25:**192–205.
44. **van der Spoel, D., E. Lindahl, B. Hess, G. Groenhof, A. E. Mark, H. J. Berendsen.** 2005. GROMACS: fast, flexible, and free. J. Comput. Chem. **26:**1701–1718.
45. **van Gunsteren, W. F., S. R. Billeter, A. A. Eising, P. H. Hunenberger, P. Kruger, A. E. Mark, W. R. P. Scott, and I. G. Tironi.** 1996. Biomolecular simulation: the GROMOS96 manual and user guide. ETH, Zürich, Switzerland.
46. **Vila-Coro, A. J., M. Mellado, A. Martin de Ana, P. Lucas, G. del Real, A. C. Martinez, and J. M. Rodriguez-Frade.** 2000. HIV-1 infection through the CCR5 receptor is blocked by receptor dimerization. Proc. Natl. Acad. Sci. USA **97:**3388–3393.
47. **Wishart, D. S., B. D. Sykes, and F. M. Richards.** 1992. The chemical shift index: a fast and simple method for the assignment of protein secondary structure through NMR spectroscopy. Biochemistry **31:**1647–1651.
48. **Wütrich, K.** 1986. NMR of proteins and nucleic acids. Wiley, New York, NY.
49. **Zhang, Y., C. Pool, K. Sadler, H. P. Yan, J. Edl, X. Wang, J. G. Boyd, and J. P. Tam.** 2004. Selection of active ScFv to G-protein-coupled receptor CCR5 using surface antigen-mimicking peptides. Biochemistry **43:**12575–12584.
50. **Zhu, L., M. C. van de Lavoir, J. Albanese, D. O. Beenhouwer, P. M. Cardarelli, S. Cuison, D. F. Deng, S. Deshpande, J. H. Diamond, L. Green, E. L. Halk, B. S. Heyer, R. M. Kay, A. Kerchner, P. A. Leighton, C. M. Mather, S. L. Morrison, Z. L. Nikolov, D. B. Passmore, A. Pradas-Monne, B. T. Preston, V. S. Rangan, M. Shi, M. Srinivasan, S. G. White, P. Winters-Digiacinto, S. Wong, W. Zhou, and R. J. Etches.** 2005. Production of human monoclonal antibody in eggs of chimeric chickens. Nat. Biotechnol. **23:**1159–1169.